

Article

Study on Pyrolysis Behaviors and Characteristics, Thermodynamics, Kinetics, and Volatiles of Single-Base Propellant, a Typical Energy-Containing Material

Yitao Liu ^{1,†}, Wenfang Zheng ^{1,†}, Yueqiang Wu ¹ and Ruiyu Chen ^{1,2,*} 

¹ School of Chemistry and Chemical Engineering, Nanjing University of Science and Technology, Nanjing 210094, China; liuyitao@njust.edu.cn (Y.L.); zhwf@njust.edu.cn (W.Z.); 122103222386@njust.edu.cn (Y.W.)

² Department of Building Environment and Energy Engineering, The Hong Kong Polytechnic University, HongKong, China

* Correspondence: crynjust@njust.edu.cn; Tel.: +86-025-8430-3159

† These authors contributed equally to this work.

Abstract: The widespread use of single-base propellant may contribute to serious pollution of the environment. The study of single-base propellant pyrolysis could provide an in-depth understanding of the combustion mechanism, reveal the key steps and reaction kinetics of the combustion process, and reduce the damage when using single-base propellant to the environment. In the present study, the pyrolysis behaviors, pyrolysis characteristic parameters, kinetics, thermodynamics, and volatiles of single-base propellant pyrolysis in an argon atmosphere were studied. The results showed that the main temperature ranges of pyrolysis and heat variation were 400–700 K and 450–520 K, respectively. With the increase in the heating rate, the maximum/average reaction rate of pyrolysis increased, the maximum instantaneous heat flow and the heat flow integral increased, the pyrolysis and combustion performance increased, and the thermal stability decreased. The average global activation energy and pre-exponential factor of the pyrolysis were 202.82 kJ and 9.48×10^{21} , respectively. Thermodynamic analysis showed that the single-base propellant pyrolysis was a spontaneous endothermic reaction with a low energy barrier and fast reaction rate, which was beneficial to the formation of active complexes. In addition, information on the main volatiles was obtained, including H₂, CH₄, C₂H₄, C₂H₆, H₂O, HCN, HCOOH, NO₂, HONO, and CO₂.

Keywords: pyrolysis; single-base propellant; energy-containing materials; kinetics; thermodynamics; volatiles



Citation: Liu, Y.; Zheng, W.; Wu, Y.; Chen, R. Study on Pyrolysis Behaviors and Characteristics, Thermodynamics, Kinetics, and Volatiles of Single-Base Propellant, a Typical Energy-Containing Material. *Fire* **2023**, *6*, 370. <https://doi.org/10.3390/fire6100370>

Academic Editor: Jianping Zhang

Received: 5 August 2023

Revised: 13 September 2023

Accepted: 21 September 2023

Published: 23 September 2023



Copyright: © 2023 by the authors. Licensee MDPI, Basel, Switzerland. This article is an open access article distributed under the terms and conditions of the Creative Commons Attribution (CC BY) license (<https://creativecommons.org/licenses/by/4.0/>).

1. Introduction

Energy-containing materials are chemical substances with high energy density and controllable energy release properties. With scientific development in this area, the application of energy-containing materials is no longer limited to the military field, but has become widely used in commercial and civilian fields [1]. Single-base propellant is a representative type of energy-containing material, whose main components are nitrocellulose and some additives, such as stabilizers, plasticizers, and anti-corrosive agents (e.g., Diphenylamine (DPA), Dibutyl phthalate (DBP), Akardite II (AK II), or Dinitrotoluene (DNT), etc.), which are used to improve the performance and stability of the propellant. Due to the high energy density, low complexity, low sensitivity, and ability to release a large amount of energy during combustion, single-base propellant is widely used and plays a significant role in many fields. For example, single-base propellants are commonly used as the primary propellant in solid rocket engines, which are suitable for spacecraft and missiles with various ranges, payloads, and mission requirements [2]. Furthermore, single-base propellants can be used in tank shells, artillery ammunition, and other military applications. Their high energy

output and reliable combustion characteristics make them a vital component of ballistic weapon systems [3]. Moreover, single-base propellants are often used in various civilian explosive devices. Their high energy density and controllable combustion behavior make them widely applicable in blasting, demolition, and cinematography work [4]. Last but not least, single-base propellants are widely used for ignition power in the airbag systems of transportation vehicles [5].

However, it is worth noting that the combustion process of single-base propellant may be harmful to the environment. Small solid particles and aerosols are produced during the combustion process of single-base propellant. These volatiles not only emit suffocating odors, but may also enter rivers in the form of surface runoff or precipitation, resulting in pollution of water resources and harmful effects on aquatic ecosystems. In addition, the combustion of single-base propellant produces tail flames and exhaust gases, including carbon dioxide, water vapor, nitrogen oxides (NO_x), and carbon monoxide. Some of these gases are greenhouse gases and may have adverse effects on the global climate. Nitrogen oxides and carbon monoxide may reduce air quality, leading to acid rain and air pollution issues. When the burning residues of single-base propellant fall to the ground, the chemicals in the residues seep into the soil or groundwater, which may lead to environmental problems such as the contamination of soil and the destruction of ecosystems in the region. All the above hazards to water resources, soil resources, and atmospheric resources will ultimately impact human health, and may even increase susceptibility to issues such as cardiovascular disease, goiter, and cancer [6]. Therefore, the investigation of the combustion mechanism and the prediction of the reaction products of single-base propellant are of great significance.

Pyrolysis is the step prior to combustion. Complex organic molecules can be pyrolyzed into simple products such as gases, small solid combustible particles, and soot, which will further participate in the combustion reactions, releasing more energy. Thus, pyrolysis determines combustion and plays a crucial role in the subsequent combustion behaviors [7–9], and pyrolysis data can be used to calculate kinetics and thermodynamics, which can also provide important information about pyrolysis. By studying the pyrolysis behaviors of single-base propellant, a deeper understanding of the combustion mechanisms and processes can be achieved, and the safety performance can be assessed, which will be helpful in optimizing the design of single-base propellant and improving combustion efficiency. By studying the heat release during the pyrolysis process of single-base propellant, preliminary guidance can be provided for evaluating the energy density, burning rate, and combustion stability. In addition, the magnitude and rate of heat release directly affect the combustion behavior of single-base propellant, so this parameter is also of great significance for controlling potential combustion and explosion risks. The results of kinetic analysis of the single-base propellant pyrolysis process can be used to reveal the key parameters of the process, such as the reaction rate, activation energy, and reaction path, so as to help predict and control combustion behaviors. Thermodynamics can provide information on the variation of thermodynamic parameters of single-base propellant at different temperatures, which is essential for evaluating stability, storage performance, and heat release capacity. In addition, through the analysis of pyrolysis products, it is possible to further investigate the degree of pollution and the influence scope of the use of single-base propellant on the atmosphere, water, and soil, to reduce the impact of the use of single-base propellant on the environment, and to formulate corresponding environmental protection strategies and measures. Therefore, it is of great significance to study the pyrolysis, heat change, kinetics, thermodynamics, and pyrolysis products of single-base propellant.

In recent years, several studies have focused on the pyrolysis, kinetics, and thermodynamics of single-base propellant and the analysis of reaction products. In order to study the thermal properties of single-base propellant, Katarzyna et al. [10] used differential scanning calorimetry (DSC) and thermogravimetric analysis (TG) to determine the basic physical properties of single-base propellant and analyze the generated phenomena. The results showed that the onset temperature (T_{onset}), maximum temperature (T_{max}), and mass loss

(m) of single-base propellant pyrolysis were 445.4 K, 456.8 K, and 82.15%, respectively. In addition, the mass loss of single-base propellant during pyrolysis was independent of the type and dosage of additives. This paper only provided a simple description and analysis of the pyrolysis behaviors of single-base propellant, and the application significance in practical scenarios still needs to be explored. Jelisivac et al. [11] used a kinetic model derived from the Arrhenius equation to perform kinetic calculations of the pyrolysis process of a stabilizer (Diphenylamine (DPA)) in single-base propellant. The results showed that the pyrolysis experimental data and performance at high concentrations of DPA could be well characterized by a first-order reaction. However, only the pyrolysis kinetics of the stabilizer in single-base propellant was considered; the global kinetic parameters of single-base propellant were not calculated. In order to study the stability of single-base propellant in service, Bohn et al. [5] used the all-temperature fits method to calculate the activation energy of additives in the pyrolysis process of three different single-base propellants and predicted the corresponding possible service times. The results showed that when the single-base propellant contained 0.74 mass-% DPA and 0.48% Akardite II (AK II), the pyrolysis activation energy released by DPA and Ak II was 135.5 kJ/mol and 142.1 kJ/mol, respectively, and the possible service life was 15 years. When the single-base propellant contained 1.25 mass-% and 2.04 mass-% Ak II, respectively, the pyrolysis activation energy released by Ak II was 144.1 kJ/mol and 140.0 kJ/mol, respectively, and the possible service life was 20 years and 27 years, respectively. It is worth noting that another important parameter of the kinetics, the pre-exponential factor A , was not derived in this paper. Via and Taylor [12] employed mass spectrometry to study the composition of volatiles during the pyrolysis of single-base propellant. The results indicated that the volatiles were composed of substances such as DPA, *N*-NO-DPA, 2,4-Dinitrotoluene (DNT), 2-N-DPA, 4-N-DPA, and 2,2'-introDPA. However, this paper only made a brief analysis of the pyrolysis volatiles of single-base propellant, without in-depth and specific estimation of the gas composition. Therefore, there are still some deficiencies in the existing articles in revealing the mechanisms of pyrolysis, kinetics, thermodynamics, and volatiles of single-base propellant.

In order to conduct in-depth research and analysis on the above problems, in the present study, simultaneous thermal analysis experiments of thermogravimetric–differential calorimetric scanning of single-base propellant were carried out with four heating rates in an argon-filled environment. The variation characteristics of mass and heat during pyrolysis and the pyrolysis characteristic parameters were obtained based on the experimental data. In addition, a classical kinetic method was used to calculate two important kinetic parameters in the pyrolysis process of single-base propellant: the global activation energy E and the pre-exponential factor A . The thermodynamic characteristics of the single-base propellant pyrolysis were evaluated, and the thermodynamic parameters were calculated. Last but not least, Fourier transform infrared spectroscopy and mass spectrometry were selected to analyze the composition of volatiles in the pyrolysis process of single-base propellant in detail.

2. Experimental and Theoretical Background

2.1. Experimental

2.1.1. Materials

The single-base propellant used in the experiments and analyses were all industrial raw materials from the unified production batch, which were composed of 89.8% nitrocellulose and 10.2% DBP. The detailed performance parameters that were tested are listed in Table 1. In addition, in order to further verify the percentage of various elements in the samples, elemental analysis was performed by an elemental analyzer (Elementar Vario EL cube), and the detailed data obtained are shown in Table 2.

Table 1. The performance parameters of single-base propellant.

Project	Single-Base Propellant
Apparent density/kg m ⁻³	600
Acidity/%	0.03
Ignition point/°C	174
Viscosity/Pa s	5.2
80 °C Thermal resistance test/K W ⁻¹	>15

Table 2. The percentage of various elements in single-base propellant.

Single-base propellant	Elemental analysis (wt.% dry ash free)			
	N	C	H	O
	9.75	32.56	4.22	9.82

2.1.2. Thermogravimetric and Differential Scanning Calorimetry Analysis

The TG and DSC experiments were carried out synchronously and jointly by the Nechi STA 449 F3 Jupiter synchronous thermal analyzer from Germany to track the changes in mass and heat of single-base propellant with temperature and heating rate in real time [13,14]. In the experiments, the temperature was increased from 300 K to 1000 K at the heating rate of 5, 10, 15, and 20 K/min, respectively [15,16]. The filling gas of the synchronous thermal analyzer was argon gas with a purity of 99.99%. In the sample preparation stage before the experiment, samples were repeatedly weighed three times to ensure that the quality was controlled at 3.5 mg (± 0.05 mg).

2.1.3. Fourier Transform Infrared Spectroscopy Analysis

The Thermo-fisher-is 50 Fourier transform infrared (FTIR) spectrometer was connected to the end of the synchronous thermal analyzer by a gas transmission line to receive and identify the volatiles generated by the pyrolysis of single-base propellant. The spectral range of the spectrometer was set to 4000–5000 cm⁻¹, the resolution was set to 0.09 cm⁻¹, and the scanning speed was set to 0.158 cm/s [17].

2.1.4. Mass Spectrographic Analysis

The NETZSCH-QMS403D gas chromatography–mass spectrometry was connected to the end of the infrared spectrometer through a quartz gas transmission line to further quantitatively analyze the composition of volatiles. The ionization voltage of the equipment was adjusted to 70 eV and the scanning speed was adjusted to 0.2 s [18].

2.2. Theoretical Background

2.2.1. Kinetic Methods

Kinetic analysis mainly focuses on the rate and reaction mechanism in the process of material and energy conversion, which plays an important role in the study of solid combustible pyrolysis [19,20], and provides an important theoretical basis in the fields of catalyst design, reaction optimization, environmental protection, and energy conversion [21–23]. The pyrolysis kinetic equation of single-base propellant can be mathematically characterized by Equations (1) and (2). Equations (3) and (4) are supplementary to Equation (1).

$$\frac{d\alpha}{dt} = \kappa f(\alpha) \quad (1)$$

$$g(\alpha) = \int_0^\alpha \frac{d\alpha}{f(\alpha)} = \frac{A}{\beta} \int_0^{T_\alpha} \exp\left(-\frac{E}{RT}\right) dT = \frac{AE}{R\beta} \int_{y_\alpha}^\infty \frac{\exp(-y)}{y^2} dy \quad (2)$$

$$\kappa = A \exp\left(-\frac{E}{RT}\right) \quad (3)$$

$$f(\alpha) = (1 - \alpha)^n \tag{4}$$

In the above equations, $f(\alpha)$ and $g(\alpha)$ represent expressions for the differential and integral forms of the kinetic reaction model, respectively. R is the general gas constant, which is 8.314 J/(mol·K). T is the transient temperature of the sample. E and A are the activation energy and the pre-exponential factor, respectively, which are the key objects of interest in kinetic analysis. α and β are the conversion rate and the heating rate, respectively, both of which are important independent variables in thermal analysis experiments and kinetic analyses. In addition, $y_\alpha = E_\alpha/RT$, $y = E/RT$.

The Kissinger method has the characteristic of not relying on specific reaction mechanisms or model assumptions [24,25]. Therefore, it is applicable to the kinetic calculations of various types of pyrolysis reactions, including complex multi-step reactions. In the present paper, the Kissinger method was chosen to estimate the kinetic parameters (such as activation energy E and pre-exponential factor A) during the pyrolysis process of single-base propellant. The expression equation of this method is as follows.

Equation (5) can be obtained from Equations (1), (3), and (4), as shown below.

$$\frac{d\alpha}{dt} = A \exp\left(-\frac{E}{RT}\right)(1 - \alpha)^n \tag{5}$$

By differentiating on both sides of Equation (5), the following results are obtained.

$$\begin{aligned} \frac{d}{dt} \left[\frac{d\alpha}{dt} \right] &= \left[A(1 - \alpha)^n \frac{d \exp\left(-\frac{E}{RT}\right)}{dt} + A \exp\left(-\frac{E}{RT}\right) \frac{d(1 - \alpha)^n}{dt} \right] \\ &= \frac{d\alpha}{dt} \frac{E}{RT^2} \frac{dT}{dt} - A \exp\left(-\frac{E}{RT}\right) n(1 - \alpha)^{n-1} \frac{d\alpha}{dt} \\ &= \frac{d\alpha}{dt} \left[\frac{E}{RT^2} \frac{dT}{dt} - An(1 - \alpha)^{n-1} \exp\left(-\frac{E}{RT}\right) \right] \end{aligned}$$

when $T = T_p$, $\frac{d}{dt} \left[\frac{d\alpha}{dt} \right] = 0$. Therefore, the above equation can be changed into the following form.

$$\frac{E}{RT_p^2} \frac{dT}{dt} = An(1 - \alpha_p)^{n-1} \exp\left(-\frac{E}{RT_p}\right) \tag{6}$$

Kissinger believes that $n(1 - \alpha_p)^{n-1}$ is independent of β , which is approximately equal to 1. Thus, Equation (6) can be evolved into Equation (7).

$$\frac{E\beta}{RT_p^2} = A \exp\left(-\frac{E}{RT_p}\right) \tag{7}$$

Taking logarithms on both sides of Equations (7) and (8) can be obtained, which is the Kissinger equation.

$$\ln\left(\frac{\beta_i}{T_{p_i}^2}\right) = \ln \frac{A_\kappa R}{E_\kappa} - \frac{E_\kappa}{R} \frac{1}{T_{p_i}} [i = 1, 2, 3, \dots] \tag{8}$$

2.2.2. Calculation of Pyrolysis Characteristic Parameters

Pyrolysis characterization parameters (D) are quantitative data used to measure the feasibility and thermal stability of solid combustibles pyrolysis and to explore the level of pyrolysis [26–28]. In the present paper, the detailed characteristics of single-base propellant pyrolysis at different heating rates could be presented through this data. The calculation equation of D is shown in Equation (9), where T_i and T_{max} represent the initial pyrolysis temperature and the peak temperature, respectively, and $T_{1/2}$ is the temperature interval

when $(dw/dt)/(dw/dt)_{max} = 1/2$. In addition, the meaning of $(dw/dt)_{max}$ is the maximum rate of mass loss, while the meaning of $(dw/dt)_{mean}$ is the average rate of mass loss.

$$D = \frac{\left(\frac{dw}{dt}\right)_{max} \left(\frac{dw}{dt}\right)_{mean}}{T_i T_{max} T_{1/2}} \quad (9)$$

2.2.3. Calculation of Thermodynamics

The results of thermodynamic analysis have a wide application value. Enthalpy and entropy are important physical quantities to describe the thermodynamic system, which together determine the thermal effect and spontaneity of the reaction. Enthalpy describes the thermal energy changes of the system, and entropy reveals the change of the disorder degree of the system. Through the analysis of enthalpy and entropy, we can gain insight into the properties of thermodynamic processes and chemical reactions, so as to provide support for the research of material properties, reaction mechanisms, and the optimization of process conditions [29]. The equations for the above parameters are shown in Equations (10) and (11), where T_m is the maximum temperature during the reaction, A is obtained based on the Kissinger method, h is the Planck constant with a value of 6.626×10^{-34} J·s, and K_B is the Boltzmann constant of 1.381×10^{-23} J/K.

$$\Delta H = E_\alpha - RT_\alpha \quad (10)$$

$$\Delta S = -(RT_\alpha + RT_m \ln\left(\frac{K_B T_m}{hA}\right))/T_m \quad (11)$$

3. Analyses and Discussion of Results

3.1. The Analysis of Thermogravimetric Experiments

Thermogravimetric (TG) analysis can be used to determine the pyrolysis characteristics of single-base propellant, including information on the pyrolysis temperature range, weight loss, and weight loss rate. These data are helpful in understanding the mass changes that occur in single-base propellant during the heating process, to determine the thermal stability and reactivity, and to determine potential safety risks.

The pyrolysis curves (reaction rate and conversion rate curves) of single-base propellant heated in an argon atmosphere with heating rates of 5, 10, 15, and 20 K/min are shown in this section (Figure 1). The trends and laws of the pyrolysis process can be obtained intuitively by analyzing the curves, and more detailed data are listed in Table 3 to further reveal the pyrolysis mechanism of single-base propellant.

Table 3. Details of single-base propellant pyrolysis.

Heating Rate (K/min)	Maximum Reaction Rate (K ⁻¹)	Temperature Corresponding to Maximum Reaction Rate (K)	Conversion Rate Corresponding to Maximum Reaction Rate	Average Reaction Rate (K ⁻¹)	Temperature Corresponding to the Turning Point (K)	Main Pyrolysis Temperature Range
5	3.34×10^{-2}	476.33	0.36	1.76×10^{-3}	510 K	400–700 K
10	3.55×10^{-2}	482.51	0.36	1.78×10^{-3}	510 K	
15	3.76×10^{-2}	485.95	0.40	1.81×10^{-3}	510 K	
20	4.00×10^{-2}	489.23	0.46	1.82×10^{-3}	510 K	

As shown in Figure 1, the change in heating rate had no effect on the overall trends of both kinds of curves but, rather, affected (increased or decreased) the slope of the conversion rate curves in certain temperature intervals by changing the reaction rate. In addition, the pyrolysis of single-base propellant started at approximately 400 K and continued until approximately 700 K.

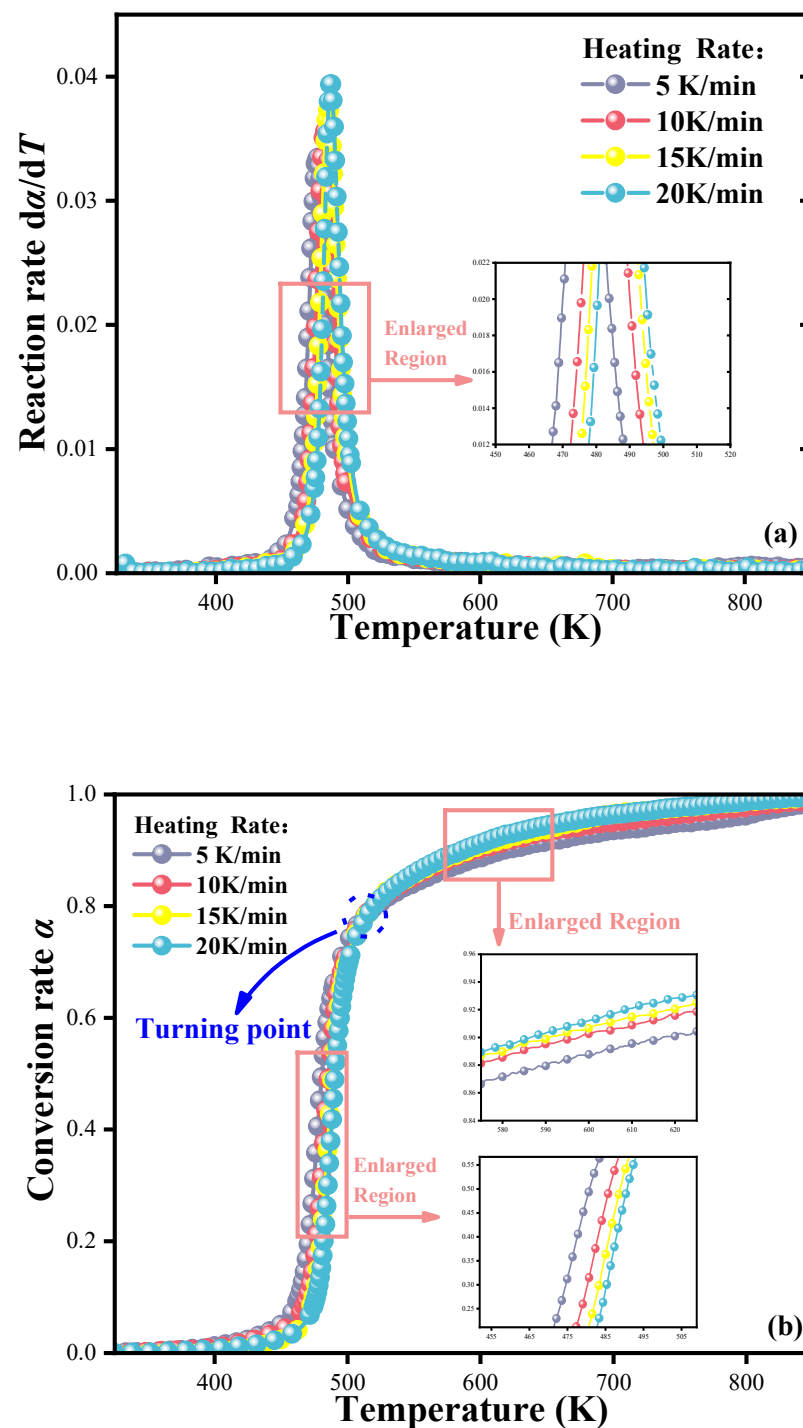


Figure 1. The pyrolysis curves of single-base propellants: (a) the reaction rate curves, (b) the conversion rate curves.

Through the analysis of the reaction rate curves, we learned that the reaction rate in the single-base propellant pyrolysis process increased rapidly to the peak value at first (for the heating rates of 5, 10, 15, and 20 K/min, the peak reaction rates were $3.34 \times 10^{-2} \text{ K}^{-1}$, $3.55 \times 10^{-2} \text{ K}^{-1}$, $3.76 \times 10^{-2} \text{ K}^{-1}$, and $4.00 \times 10^{-2} \text{ K}^{-1}$, respectively) and then dropped sharply with increasing temperature. The change in heating rate affected the reaction rate significantly, which in turn changed the slope of the conversion rate curves. As can be seen in Figure 1a, the increasing heating rate caused a clear shift of the reaction rate curve to the higher temperature area. The reason for this phenomenon can be explained by the temperature lag caused by the gradual failure of the heat transfer rate in the sample to keep

up with the programmed temperature rise rate provided by the thermogravimetric analyzer, which is known as the “temperature hysteresis phenomenon” in pyrolysis experiments.

Through the analysis of the conversion rate curves, we learned that the conversion rate of single-base propellant pyrolysis increased continuously with the increasing temperature, and the overall curves were smooth and consistent. It is worth noting that there was a turning point on the conversion curve. When the experimental temperature was less than the turning point temperature, the conversion rate corresponding to the working condition with a lower heating rate was higher at the same temperature. On the contrary, the conversion rate corresponding to the working condition with a higher heating rate was higher, and the temperature at which the turning point occurred was measured to be 510 K.

The pyrolysis process of single-base propellant could be further analyzed by the data in Table 3. With the increasing heating rate, both the maximum and average reaction rates of the pyrolysis increased, which may be attributed to the increase in excited state concentration, the enhancement of mass transfer, and thermal conduction effects. With the increase in the heating rate, the temperature corresponding to the maximum reaction rate moved to the higher temperature area, and the conversion rate corresponding to the maximum reaction rate increased.

3.1.1. The Analysis of Pyrolysis Characteristic Parameters

Table 4 gives the pyrolysis characteristic parameters (D) of single-base propellant at heating rates of 5, 10, 15, and 20 K/min. It can be seen that the pyrolysis characteristic parameters were significantly changed with the increasing heating rate. When the heating rate of pyrolysis increased from 5 K/min to 20 K/min, the initial pyrolysis temperature and the temperature corresponding to the maximum reaction rate both moved towards the higher temperature zone, which was in accordance with the characteristics of the temperature hysteresis phenomenon mentioned in the previous section. In addition, the increase in heating rate caused a decrease in the width of the half-peak temperature ($T_{1/2}$) and increases in the values of $(dw/dt)_{max}$ and $(dw/dt)_{mean}$. Eventually, the above changes were reflected in the values of D , which increased significantly. The changes in $T_{1/2}$ showed that the thermal conduction and mass transfer process in the sample plays an important role in the pyrolysis reaction, and the changes in pyrolysis characteristic parameters were consistent with the results obtained by TG analysis. When the heating rate increased, the thermal stability of the single-base propellant decreased significantly, and the pyrolysis and combustion performance increased significantly.

Table 4. Pyrolysis characteristic parameters (D).

β (K/min)	T_i (K)	T_{max} (K)	$T_{1/2}$ (K)	$(dw/dt)_{max}$ (% min ⁻¹)	$(dw/dt)_{mean}$ (% min ⁻¹)	D ($\times 10^{-13}$)
5	460.47	476.33	18.98	1.63×10^{-3}	0.82×10^{-3}	3.2107
10	465.48	482.51	18.19	1.71×10^{-3}	0.91×10^{-3}	3.8089
15	470.99	485.95	17.38	2.21×10^{-3}	0.92×10^{-3}	5.1113
20	471.79	489.23	16.43	3.27×10^{-3}	0.94×10^{-3}	8.1054

3.1.2. The Analysis of Differential Scanning Calorimetry

Differential scanning calorimetry (DSC) analysis can be used to determine the thermal effect of single-base propellant, including the changes in heat release or absorption. This is of great significance for evaluating the combustion performance, explosion performance, and safety of single-base propellant. The violent reactions that occur in energy-containing materials at high temperatures are often accompanied by uncontrolled energy release. Therefore, understanding the heat changes during the pyrolysis process of single-base propellant is crucial for its safe design and operation.

The results of DSC tests of single-base propellant in an argon atmosphere at heating rates of 5, 10, 15, and 20 K/min are presented in this section. Figure 2 shows the heat flow variation curves and the total heat release during the single-base propellant pyrolysis

process, from which the changes in heat could be intuitively observed. The important characteristic parameters of heat variation are shown in Table 5. Combining the DSC data with the analysis results of the thermogravimetric (TG) data in the previous section, the characteristics of single-base propellant pyrolysis could be further determined, and important clues about the thermal stability and reaction activity of single-base propellant could also be obtained.

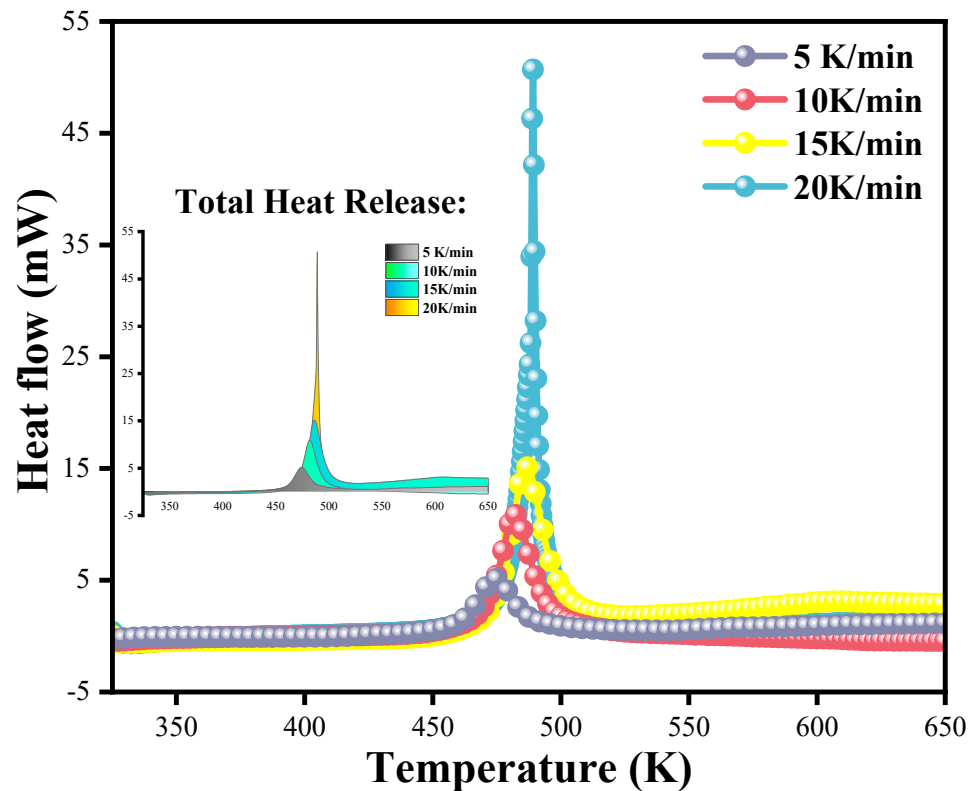


Figure 2. The heat flow variation curves and the total heat release of the single-base propellant.

Table 5. The characteristic parameters of heat variation.

Heating Rate β (K/min)	Maximum Instantaneous Heat Flow (mW)	Temperature Corresponding to Maximum Instantaneous Heat Flow (K)	Integral of Heat Flow (mJ)	FWHM	Main Heat Variation Range
5	4.77	474.40	92.79	16.13	450–520 K
10	11.22	482.15	116.23	15.34	
15	13.74	486.40	138.00	13.78	
20	49.92	489.15	182.55	2.24	

Through the analysis of the heat flow curves and the total heat release figure, it can be seen that when the temperature reached approximately 450 K, the heat release of single-base propellant pyrolysis started to rise and rapidly reached the peak value (the maximum instantaneous heat flow at heating rates of 5, 10, 15, and 20 K/min were 4.77, 11.22, 13.74, and 49.92 mW, respectively) and then began to decrease rapidly. When the temperature reached approximately 520 K, the heat release rate was essentially stable. Subsequently, as the temperature increased, the heat was released slowly at an almost steady rate until the end of the reaction. According to the variation of heat release mentioned above, the pyrolysis of single-base propellant mainly occurred after the temperature of 450 K. The temperature range of 450–520 K was the main reaction range, in which the heat was released rapidly and the reaction occurred violently. Therefore, it can be inferred that the pyrolysis

of nitrocellulose (NC), the main component of single-base propellant, mainly occurs in this temperature range. In addition, a small amount of heat was released continuously after the temperature exceeded 520 K, and it can be inferred that the pyrolysis of the additives or binder components of single-base propellant occurred during this time.

With the help of Table 5, the changes in heat flow during single-base propellant pyrolysis can be understood in detail. It can be seen that as the heating rate increased, the full width at half maximum (FWHM) of the heat flow curve decreased (for the heating rates of 5, 10, 15, and 20 K/min, the FWHM were 16.13, 15.34, 13.78, and 2.24, respectively), and the maximum instantaneous heat flow increased, which indicated that increasing the heating rate of single-base propellant pyrolysis can cause the heat release to occur more quickly, in a shorter period of time; that is, it can increase the intensity of the reaction. The change in FWHM indicated that the reaction may have been more complex at a lower heating rate, while a higher heating rate may have led to a more concentrated reaction. In addition, a higher heating rate may reduce the localized temperature and concentration gradients, making the reaction more uniform. This further indicated that this material is sensitive to temperature changes, with the reaction rate being slower at lower temperatures and becoming violent at higher temperatures. The above results could be confirmed by the total heat release (integral of heat flow): an increasing heating rate led to the increase in total heat release from 92.79 at 5 K/min to 182.55 at 20 K/min.

It is worth noting that, similar to the results obtained in TG analysis, the temperature hysteresis phenomenon also occurred in the DSC. It can be observed from Figure 2 and Table 5 that the temperature corresponding to the maximum instantaneous heat flow and the overall temperature of the heat flow curve moved to the higher temperature region with the increase in the heating rate. This corresponds to the findings of the previous section, indicating that the analysis of TG and DSC was accurate and reliable.

3.2. The Analysis of Kinetics

Studying the kinetics of pyrolysis processes allows us to analyze substances from a more comprehensive perspective. The study on the kinetics of single-base propellant pyrolysis could lead to a deeper understanding of the mechanism and details of the reaction, improve safety, and optimize the reaction conditions. This could provide a scientific basis and technical support for the application and development of single-base propellant. Therefore, the calculation and analysis of kinetics are of great significance.

There are two parameters of notable importance in kinetics, which are the activation energy E and pre-exponential factor A . The activation energy is an important parameter used to describe the energy barrier of a chemical reaction. According to the Arrhenius equation [30], the relationship between the reaction rate constant and temperature can be described by the activation energy. A lower activation energy means that the energy barrier is more easily overcome and the reaction rate is faster, while a higher activation energy indicates a slower reaction rate.

The pre-exponential factor is the pre-coefficient of the reaction rate constant, reflecting the possibility of pyrolysis and the reaction rate of solid materials within a certain temperature range. A larger pre-exponential factor means a faster reaction rate, while a smaller one means a slower reaction rate. In addition, the pre-exponential factor can provide information about the reaction mechanism. Generally speaking, reactions with a larger pre-exponential factor tend to have a simpler mechanism, while a smaller pre-exponential factor suggests more complex steps and processes may be involved. In summary, the study of the activation energy and pre-exponential factor has important practical significance and theoretical value. Therefore, these two parameters of single-base propellant pyrolysis were investigated in detail in this section.

The Kissinger method was used in this section to calculate the activation energy and pre-exponential factor of the pyrolysis process of single-base propellant at the heating rates of 5, 10, 15, and 20 K/min. The activation energy and pre-exponential factor could be calculated from the slope and intercept of the fitted curve of $1/T_{pi}$ and $\ln(\beta/T_{pi}^2)$,

respectively, as shown in Figure 3. Table 6 shows the detailed results of the calculation, with an activation energy of 202.82 kJ and a pre-exponential factor of 9.48×10^{21} , which indicated that the pyrolysis of single-based propellants reacted at a relatively fast rate and was sensitive to temperature. It is worth noting that the correlation coefficient R^2 of the fitted curve was extremely high, so it can be considered that the kinetic results were accurate and could be used under a wider range of conditions.

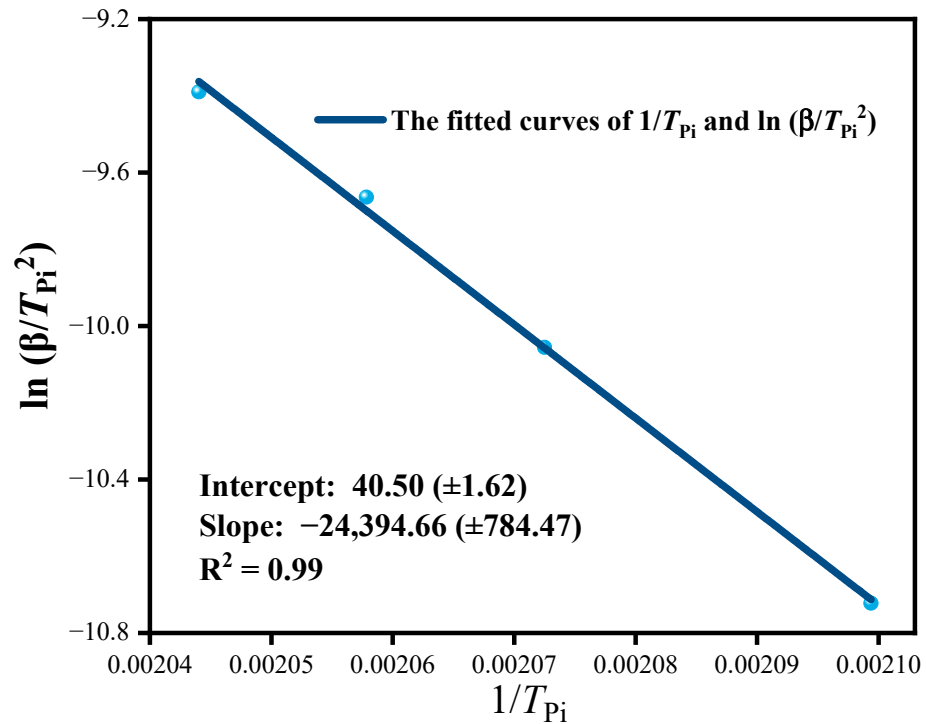


Figure 3. The fitted curve of $1/T_{pi}$ and $\ln(\beta/T_{pi}^2)$.

Table 6. The detailed results of the Kissinger method.

Heating Rate β (K/min)	T_{pi}	$\ln(\beta/T_{pi}^2)$	$1/T_{pi}$	Intercept	Slope	E (kJ)	A	R^2
5	476.33	-10.72	2.10×10^{-3}	40.50	-24,394.66	202.82	9.48×10^{21}	0.99
10	482.51	-10.06	2.07×10^{-3}					
15	485.95	-9.66	2.06×10^{-3}					
20	489.23	-9.39	2.04×10^{-3}					

3.3. Uncertainty Analysis

For the kinetic calculations, the input parameters of the heating rate (β) and peak temperature (T_{pi}) may deviate due to external factors or instrument limitations, which can affect the calculation results of the E value. Taking into account the actual conditions of the experimental instrument, we set the actual values of each group of β and T_{pi} with uncertainty deviations as randomly distributed within the range of $\beta \pm 0.1$ K/min and $T_{pi} \pm 5$ K, respectively. With the help of Monte Carlo simulation and Equation (8), we conducted 10,000 calculations of sample data and obtained parameters such as the mean, variance, and probability distribution, as shown in Figure 4 and Table 7.

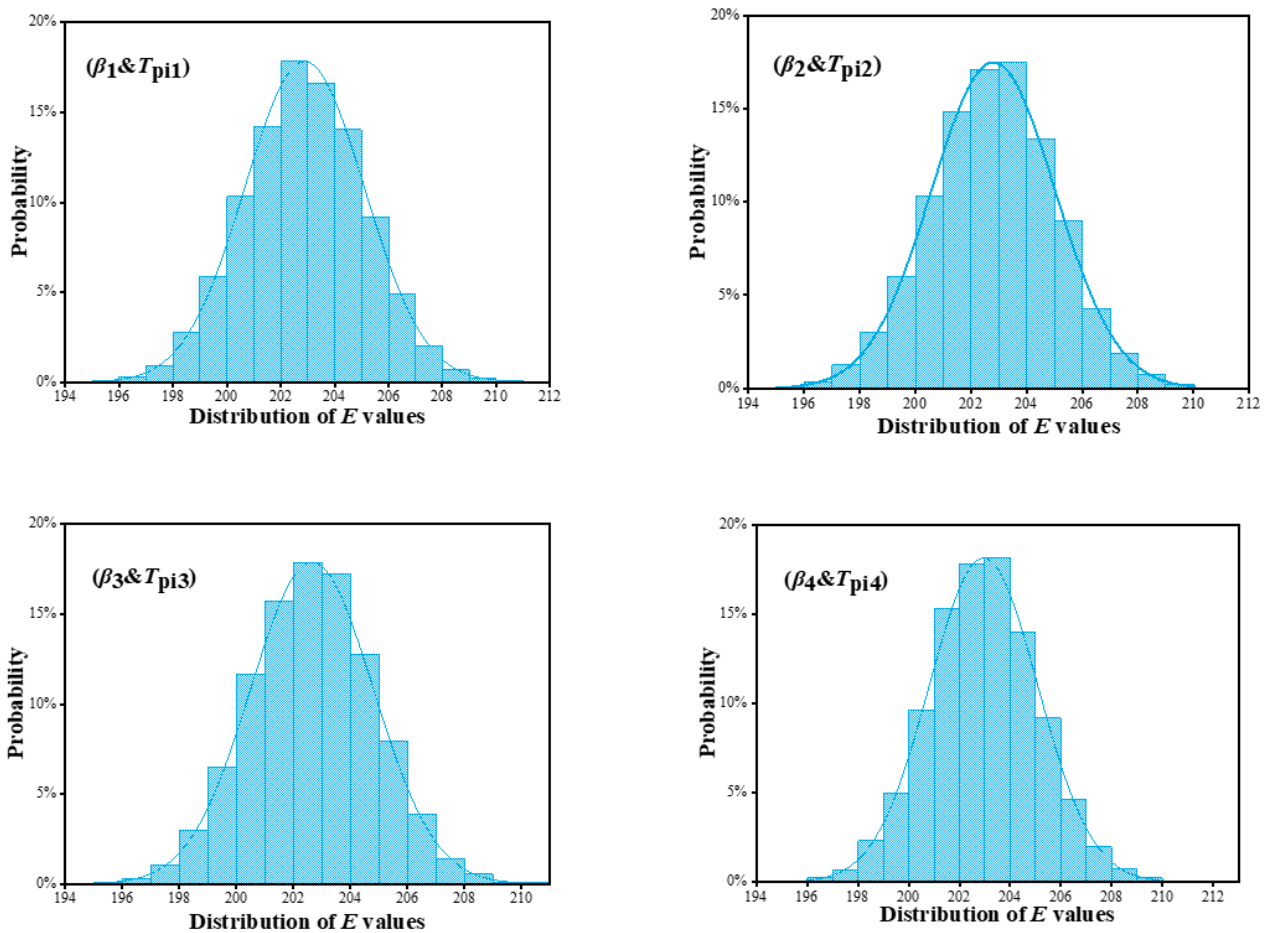


Figure 4. The probability distribution of the E value.

Table 7. Uncertainty analysis results.

Simulated Working Condition	β_1 & T_{pi1}	β_2 & T_{pi2}	β_3 & T_{pi3}	β_4 & T_{pi4}
Average value (kJ)	202.88	202.79	202.65	202.95
Standard deviation	4.94	4.95	4.62	4.57
Uncertainty degree (%)	2.43	2.44	2.23	2.22

According to the results, the uncertainty variations in β and T_{pi} had a negligible impact on E (the uncertainties under the four simulated conditions were 2.43%, 2.44%, 2.23%, and 2.22%, respectively). Furthermore, the average E values calculated using the Monte Carlo model under the four conditions were extremely close to the 202.82 kJ obtained by the Kissinger method, which indicated that the calculated activation energy results in this study were accurate and reliable.

3.4. The Analysis of Thermodynamics

Thermodynamic analysis can be used to study energy transformations, phase transitions, and equilibrium behaviors of substances under different conditions. Through this method, the basic thermodynamic principles of the pyrolysis reaction could be revealed, the efficiency and possibilities of the pyrolysis reaction could be evaluated, the temperature effect of the pyrolysis reaction could be analyzed, and the reaction conditions could be optimized. This section analyzed the variation of thermodynamic parameters with the conversion rate during pyrolysis of single-base propellant at heating rates of 5, 10, 15, and 20 K/min, as shown in Figure 5. More detailed calculations are presented in Table 8.

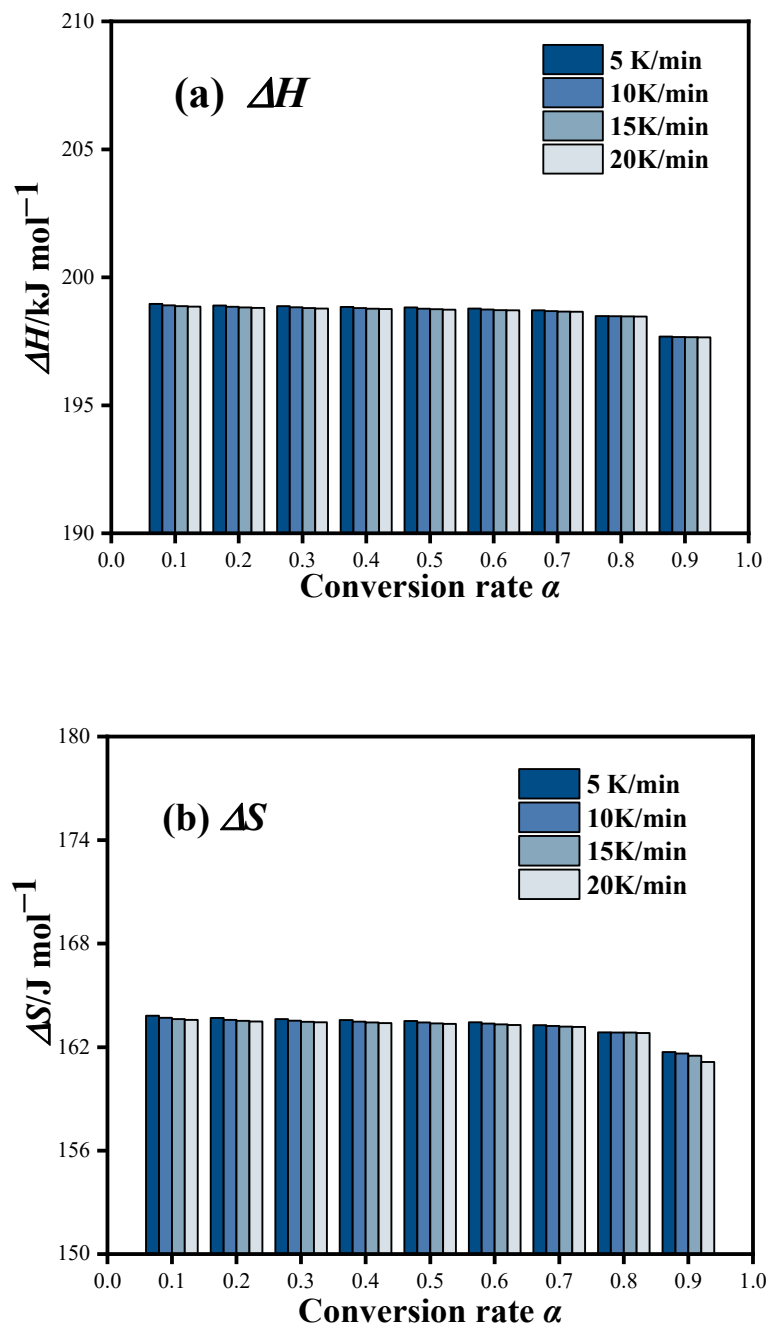


Figure 5. The variation of the (a) ΔH and (b) ΔS .

Table 8. The detailed results of the thermodynamic analysis.

Conversion Rate	ΔH (kJ/mol)				ΔS (J/mol)			
	5 K/min	10 K/min	15 K/min	20 K/min	5 K/min	10 K/min	15 K/min	20 K/min
0.05	199.08	199.02	198.95	198.94	164.06	163.94	163.77	163.76
0.1	198.96	198.91	198.87	198.85	163.82	163.70	163.62	163.58
0.15	198.93	198.87	198.84	198.82	163.74	163.63	163.56	163.52
0.2	198.90	198.85	198.83	198.81	163.69	163.58	163.53	163.49
0.25	198.89	198.84	198.81	198.79	163.65	163.55	163.50	163.46
0.3	198.87	198.83	198.80	198.78	163.63	163.53	163.47	163.44
0.35	198.86	198.81	198.79	198.77	163.59	163.50	163.45	163.42

Table 8. Cont.

Conversion Rate	ΔH (kJ/mol)				ΔS (J/mol)			
	5 K/min	10 K/min	15 K/min	20 K/min	5 K/min	10 K/min	15 K/min	20 K/min
0.4	198.85	198.80	198.78	198.76	163.57	163.48	163.43	163.39
0.45	198.84	198.79	198.76	198.75	163.55	163.45	163.40	163.37
0.5	198.82	198.77	198.75	198.74	163.52	163.43	163.37	163.35
0.55	198.81	198.76	198.74	198.73	163.48	163.39	163.35	163.32
0.6	198.78	198.74	198.72	198.71	163.44	163.36	163.32	163.29
0.65	198.75	198.72	198.70	198.68	163.37	163.31	163.27	163.24
0.7	198.71	198.68	198.66	198.65	163.28	163.22	163.19	163.17
0.75	198.63	198.61	198.60	198.59	163.12	163.09	163.07	163.06
0.8	198.49	198.48	198.47	198.46	162.85	162.85	162.85	162.82
0.85	198.18	198.16	198.15	198.14	162.44	162.42	162.36	162.17
0.9	197.69	197.67	197.66	197.66	161.72	161.63	161.50	161.14
0.95	196.55	196.31	196.21	196.00	160.43	160.21	159.74	158.74
average value	198.61	198.56	198.53	198.50	163.21	163.12	163.04	162.93
		198.55				163.08		

Enthalpy change (ΔH) is a physical quantity used in thermodynamics to describe the heat absorption and release in the process of a chemical reaction or phase transformation in a system under constant pressure, which can be interpreted as the thermodynamic state of the system. A positive enthalpy change indicates that the reaction is endothermic and requires an external supply of heat to proceed, while a negative enthalpy change indicates that the reaction is exothermic, releasing heat into the surrounding environment. It can be seen from Figure 5 and Table 8 that ΔH remained positive at all heating rates and conversion rates, which indicated that the pyrolysis of single-base propellant is an endothermic reaction. When the heating rates were 5, 10, 15, and 20 K/min, the maximum values of ΔH were 199.08, 199.02, 198.95, and 198.94 kJ/mol, respectively, and the average values were 198.61, 198.56, 198.53, and 198.50 kJ/mol, respectively. In addition, a relationship exists between the activation energy E and ΔH called the energy barrier, which represents the energy difference that needs to be overcome when the system changes from one stable state to another in a chemical reaction. If the absolute value difference between the values of E and ΔH in a certain reaction is not greater than 7 kJ/mol, the reaction has a lower energy barrier and a faster reaction rate, which is beneficial to the formation of active complexes. In the present study, the difference was 4.27 kJ/mol, which was consistent with the above description.

Entropy change (ΔS) is a thermodynamic process caused by the mixing and decomposition of substances and the expansion and dissolution of gases. A positive value of entropy change indicates an increase in the disorder of the system, while a negative entropy change value indicates a decrease in the disorder of the system. As shown in Figure 5 and Table 8, the ΔS values were positive at all heating rates and conversion rates, which means that the pyrolysis products of single-base propellant were more disordered than the reactants, indicating that the pyrolysis of single-base propellant is spontaneous. When the heating rates were 5, 10, 15, and 20 K/min, the maximum values of ΔS were 164.06, 163.94, 163.77, and 163.76 kJ/mol, respectively, and the average values of ΔS were 163.21, 163.12, 163.04, and 162.93 J/mol, respectively.

3.5. Composition Analysis of Pyrolysis Volatiles

Infrared spectrum and mass spectrometry analysis were able to provide information on the composition of volatiles produced during the pyrolysis process of single-base propellant. Analyzing the structure and chemical bond properties of these products was helpful for determining the reaction mechanism and the main reaction paths of single-base propellant pyrolysis. In addition, information on dangerous and toxic substances that may be produced by single-base propellant pyrolysis at high temperatures, which pose potential

threats to human health and the environment, could also be obtained through infrared spectrum and mass spectrometry analysis.

3.5.1. Infrared Spectrum Analysis

The infrared spectrum of volatiles from thermogravimetric experiments with a heating rate of 10 K/min is presented and analyzed in detail in this section.

According to the Beer–Lambert law [31,32], the content of volatiles is directly reflected in the infrared spectrum in the form of the absorption peak intensity. We were clearly able to distinguish the following substances from Table 9 and Figure 6, among which the contents of CO₂ (2380 cm⁻¹) and NO₂ (2340 cm⁻¹) were the most abundant. The –OH stretching in H₂O was identified at 3730 cm⁻¹, 3570 cm⁻¹, and 3340 cm⁻¹. The absorption peaks at 2800 cm⁻¹ and 2200 cm⁻¹ indicated the stretching vibrations of the C–H and nitrile group (CN), respectively, and the absorption peaks at 1910 cm⁻¹ and 1740 cm⁻¹ represented the stretching vibrations of CO bonds. In addition, nitro groups (–NO₂) could be observed at the absorption peak intensity of 1510 cm⁻¹, bending vibrations of –CH could be observed at 1340 cm⁻¹, and stretching vibrations of C–O could be observed at 950 cm⁻¹. Moreover, the absorption peaks at 710 cm⁻¹ and 670 cm⁻¹ represented the deformation of O–NO, which was most likely HONO. It is noteworthy that nitrogen and carbon monoxide were hardly found in the infrared spectrum. In addition, the presence of HCN, CH₄, C₂H₄, and C₂H₆ could be inferred from the results.

Table 9. Infrared spectrum analysis of single-base propellant.

Num	Wavenumber	Substance
1	3730, 3570, 3340	–OH stretching (H ₂ O)
2	2800	C–H stretching
3	2380	CO ₂
4	2340	NO ₂
5	2200	nitrile group (–C≡N)
6	1910, 1740	C=O bond
7	1510	nitro group (–NO ₂)
8	1340	–CH bending vibrations
9	950	C–O stretching
10	710, 670	O–NO deformation (HONO)

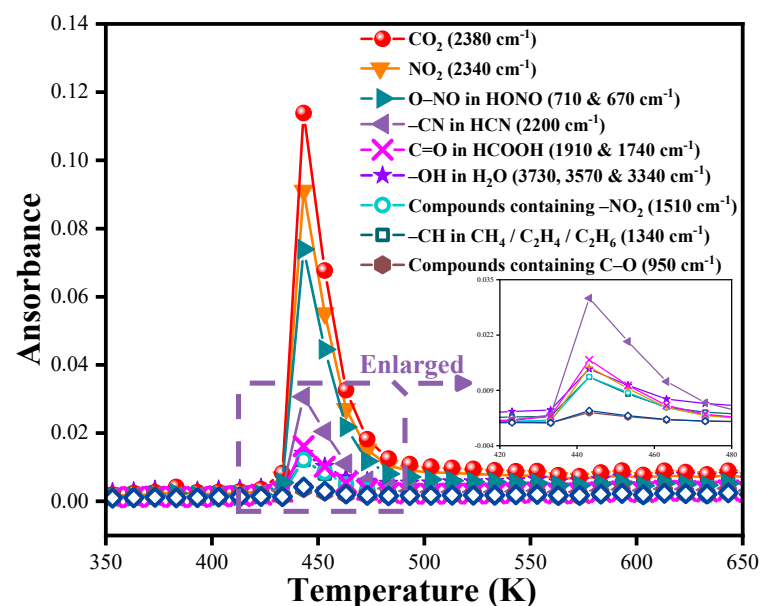


Figure 6. Evolution image of the volatiles.

3.5.2. Mass Spectrometry Analysis

The mass spectrum plotted based on the measured data is shown in Figure 7, which was processed by interference elimination and normalization, making the display effect clearer and more intuitive.

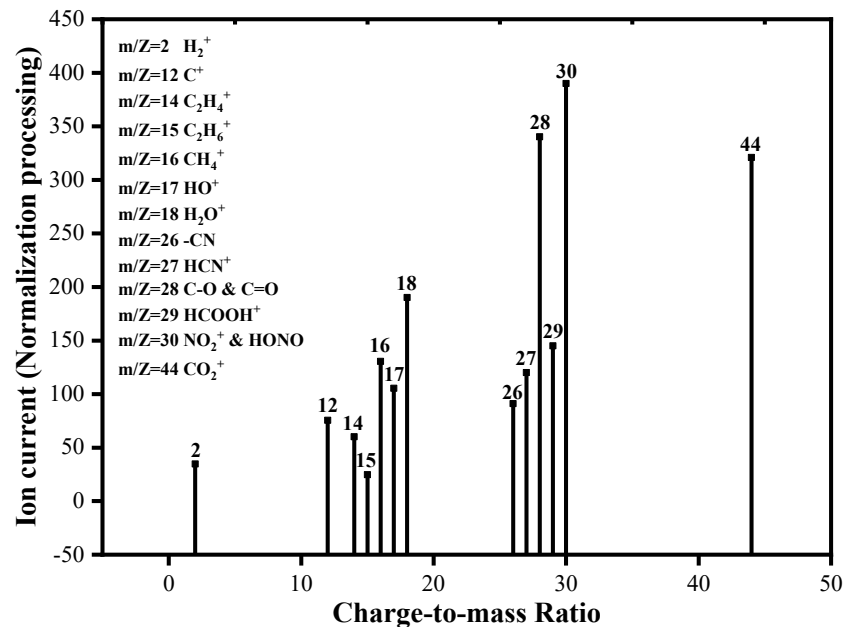


Figure 7. Mass spectrogram of the peak temperature.

Thirteen charge-to-mass ratio signals could be identified from the mass spectrogram, which were $m/z = 2, 14, 15, 16, 17, 18, 26, 27, 28, 29, 30,$ and 44 , respectively. Combining the results with those of the infrared spectrum analysis in the previous section, the composition of some volatiles could be further determined. The identification of $m/z = 2$ meant the existence of H_2 . $m/z = 12$ was the proof of the existence of C^+ . $m/z = 14, 15,$ and 16 demonstrated the presence of C_2H_4 ($=CH_2$), C_2H_6 ($-CH_3$), and CH_4 , respectively. HO^+ and H_2O could be identified from signals of $m/z = 17$ and 18 , respectively. $m/z = 26$ represented $-CN$ and $m/z = 27$ represented HCN . The existence of substances containing $C-O$ and $C=O$ in the volatiles was evidenced by $m/z = 28$, and the ion current at $m/z = 29$ indicated the existence of $HCOOH$ ($-CHO$ aldehyde group). In addition, CO_2 and NO_2 were also clearly captured in the mass spectra ($m/z = 44$, $m/z = 30$ ($-NO$)). The ion current at $m/z = 30$ also represented the existence of $HONO$. The specific comparison is shown in Table 10.

Table 10. Specific comparison table for mass spectrometry.

Num	m/z	Substance
1	2	H_2
2	12	C^+
3	14	$C_2H_4^+$
4	15	$C_2H_6^+$
5	16	CH_4^+
6	17	HO^+
7	18	H_2O^+
8	26	$-C\equiv N$
9	27	HCN
10	28	$C-O$ & $C=O$
11	29	$HCOOH$
12	30	NO_2^+ & $HONO$
13	44	CO_2^+

4. Conclusions

In the present paper, the pyrolysis behaviors, changes in mass and heat, pyrolysis characteristic parameters, kinetics, thermodynamics, and composition of volatiles of single-base propellant in an argon environment at four different heating rates were analyzed. The results obtained can provide theoretical guidance for reducing the environmental hazards caused by the use of single-base propellants. The main conclusions drawn in this paper are as follows.

1. The main temperature range of single-base propellant pyrolysis is 400–700 K. As the heating rate increased, both the reaction rate and conversion rate curves moved towards the high-temperature region, the maximum/average reaction rate and the temperature/conversion rate corresponding to the maximum reaction rate increased, the half-peak temperature decreased, and the turning point temperature remained unchanged. In addition, when the heating rate increased, the thermal stability of the single-base propellant decreased significantly, and the pyrolysis and combustion performance increased significantly.
2. The main exothermic temperature range of single-base propellant pyrolysis is 450–520 K. With the increase in the heating rate, both the maximum instantaneous heat flow and the integral of heat flow increased, and the full width at half maximum of the exothermic curve decreased.
3. The average activation energy of the pyrolysis process of single-base propellants is 202.82 kJ, and the pre-exponential factor is 9.48×10 [21].
4. The thermodynamic parameters of single-base propellant pyrolysis were obtained. The average values of ΔH and ΔS were 198.55 kJ/mol and 163.08 J/mol, respectively. This indicated that the pyrolysis of single-base propellant is an exothermic reaction with a low energy barrier and fast reaction rate, which is conducive to the formation of active complexes. In addition, the pyrolysis of single-base propellant occurs spontaneously.
5. The composition, evolution trend, and relative content of volatiles produced during the pyrolysis of single-base propellant were obtained. The main volatiles included H_2 , CH_4 , C_2H_4 , C_2H_6 , H_2O , HCN , $HCOOH$, NO_2 , $HONO$, and CO_2 , which are typical greenhouse and toxic gases. In order to reduce the adverse environmental impacts of the greenhouse gases produced, it is recommended to control the combustion process of single-base propellant, improve the combustion efficiency, and use carbon capture and storage (CCS) technology. In order to avoid environmental and biological hazards from toxic gases, the formulation of single-base propellant should be further improved, the temperature and oxidant content in the combustion process should be controlled, and exhaust gas treatment devices should be used.

5. Future Work

Given the current research status of single-base propellant, the work presented in this paper has a unique degree of innovation and practicality. The current research is considered an extremely important and yet complex problem, and there are still many areas that need to be explored and studied. Therefore, we have planned future work as follows.

1. Optimization of Combustion Efficiency

The primary reason for the widespread use of single-base propellant is its uniquely high energy output. Therefore, we intend to further optimize the combustion efficiency and enhance the propulsion performance of single-base propellant, while minimizing the environmental impact and reducing the production of harmful by-products, by exploring new additives, binder formulations, and processing techniques.

2. Establish accurate prediction models

The combustion behavior of single-base propellant is complex and poorly controllable. However, there is currently a lack of accurate predictive models. Therefore, we intend to

utilize methods such as machine learning to establish a predictive model that can accurately forecast the combustion behavior of single-base propellant.

3. More comprehensively reveal the combustion mechanism

Currently, there are few studies on the combustion mechanism and possible chemical reactions of single-base propellant. Therefore, we intend to focus on studying these aspects in our future work, aiming to promote innovation and technological advancements in this field.

Author Contributions: Conceptualization, Y.L. and W.Z.; methodology, Y.L.; validation, Y.W.; investigation, R.C.; writing—original draft preparation, Y.L.; writing—review and editing, W.Z.; visualization, Y.W.; supervision, R.C.; project administration, Yitao Liu; funding acquisition, R.C. All authors have read and agreed to the published version of the manuscript.

Funding: This work was funded by the Hong Kong Scholars Program (No. XJ2021025), the National Natural Science Foundation of China (No. 52276119), the Fundamental Research Funds for the Central Universities (No. 30922010909), China Postdoctoral Science Foundation (No. 2020M680069) and Jiangsu Planned Projects for Postdoctoral Research Funds (No. 2020Z414).

Institutional Review Board Statement: Not applicable.

Informed Consent Statement: Not applicable.

Data Availability Statement: The data presented in this study are available on request from the corresponding author.

Acknowledgments: This work was sponsored by the Hong Kong Scholars Program (No. XJ2021025), the National Natural Science Foundation of China (No. 52276119), the Fundamental Research Funds for the Central Universities (No. 30922010909), China Postdoctoral Science Foundation (No. 2020M680069), and Jiangsu Planned Projects for Postdoctoral Research Funds (No. 2020Z414).

Conflicts of Interest: The authors declare no conflict of interest.

References

1. Yu, Y.; Yang, Z.; Wang, F.; Liu, C.; Deng, L. A novel environment-friendly polyester binder to reduce the pollution of particulate matter produced by combustion of pyrotechnic. *J. Clean. Prod.* **2021**, *278*, 123733. [[CrossRef](#)]
2. Folly, P.; Mäder, P. Propellant chemistry. *Chimia* **2004**, *58*, 374. [[CrossRef](#)]
3. de Souza Defanti, B.F.; de Mendonça-Filho, L.G.; Nichele, J. Effect of ageing on the combustion of single base propellants. *Combust. Flame* **2020**, *221*, 212–218. [[CrossRef](#)]
4. Wang, P.; Wei, X.; He, W. Thermal stability and underwater energy of water gel explosive using expired single-base propellants as ingredients. *J. Energetic Mater.* **2014**, *32*, S51–S59. [[CrossRef](#)]
5. Bohn, M.A. Prediction of In-Service Time Period of Three Differently Stabilized Single Base Propellants. *Propellants Explos. Pyrotech. Int. J. Deal. Sci. Technol. Asp. Energetic Mater.* **2009**, *34*, 252–266. [[CrossRef](#)]
6. Fang, Z.; Li, S.; Liu, J. Probing the Effects of Deuteration on the Structure and Thermal Behavior of TNT-d5. *Propellants Explos. Pyrotech.* **2021**, *46*, 1581–1588. [[CrossRef](#)]
7. Kannan, P.; Biernacki, J.J.; Visco, D.P., Jr.; Lambert, W. Kinetics of thermal decomposition of expandable polystyrene in different gaseous environments. *J. Anal. Appl. Pyrolysis* **2009**, *84*, 139–144. [[CrossRef](#)]
8. Chrissafis, K.; Paraskevopoulos, K.; Papageorgiou, G.; Bikiaris, D. Thermal decomposition of poly (propylene sebacate) and poly (propylene azelate) biodegradable polyesters: Evaluation of mechanisms using TGA, FTIR and GC/MS. *J. Anal. Appl. Pyrolysis* **2011**, *92*, 123–130. [[CrossRef](#)]
9. Kruse, T.M.; Woo, O.S.; Broadbelt, L.J. Detailed mechanistic modeling of polymer degradation: Application to polystyrene. *Chem. Eng. Sci.* **2001**, *56*, 971–979. [[CrossRef](#)]
10. Gańczyk-Specjalska, K.; Cieślak, K.; Zembrzucka, K. Thermal properties of modified single-base propellants. *Mater. Wysokoenergetyczne* **2021**, *13*, 59–69. [[CrossRef](#)]
11. Jelisavac, L.; Filipović, M. Akinetic model for the consumption of stabilizer in single base gun propellants. *J. Serbian Chem. Soc.* **2002**, *67*, 103–109. [[CrossRef](#)]
12. Via, J.C.; Taylor, L.T. Chromatographic analysis of nonpolymeric single base propellant components. *J. Chromatogr. Sci.* **1992**, *30*, 106–110. [[CrossRef](#)]
13. Ding, L.; Zhao, F.Q.; Pan, Q.; Xu, H.X. Research on the thermal decomposition behavior of NEPE propellant containing CL-20. *J. Anal. Appl. Pyrolysis* **2016**, *121*, 121–127. [[CrossRef](#)]
14. Fetisova, O.Y.; Mikova, N.M.; Chudina, A.I.; Kazachenko, A.S. Kinetic Study of Pyrolysis of Coniferous Bark Wood and Modified Fir Bark Wood. *Fire* **2023**, *6*, 59. [[CrossRef](#)]

15. Ren, X.; Zong, R.; Hu, Y.; Lo, S.; Stec, A.A.; Hull, T.R. Investigation of thermal decomposition of polymer nanocomposites with different char residues. *Polym. Adv. Technol.* **2015**, *26*, 1027–1033. [[CrossRef](#)]
16. Striebich, R.; Lawrence, J. Thermal decomposition of high-energy density materials at high pressure and temperature. *J. Anal. Appl. Pyrolysis* **2003**, *70*, 339–352. [[CrossRef](#)]
17. Zhang, J.; Chen, L.; Zhao, L.; Jin, G.; He, W. Experimental insight into interaction mechanism of 1H-tetrazole and nitrocellulose by kinetics methods and TG-DSC-FTIR analysis. *J. Anal. Appl. Pyrolysis* **2023**, *169*, 105853. [[CrossRef](#)]
18. Huwei, L.; Ruonong, F. Studies on thermal decomposition of nitrocellulose by pyrolysis-gas chromatography. *J. Anal. Appl. Pyrolysis* **1988**, *14*, 163–169. [[CrossRef](#)]
19. Das, P.; Tiwari, P. Thermal degradation kinetics of plastics and model selection. *Thermochim. Acta* **2017**, *654*, 191–202. [[CrossRef](#)]
20. Paran, S.M.R.; Vahabi, H.; Jouyandeh, M.; Ducos, F.; Formela, K.; Saeb, M.R. Thermal decomposition kinetics of dynamically vulcanized polyamide 6–acrylonitrile butadiene rubber–halloysite nanotube nanocomposites. *J. Appl. Polym. Sci.* **2019**, *136*, 47483. [[CrossRef](#)]
21. Hossain, M.D.; Hassan, M.K.; Saha, S.; Yuen, A.C.Y.; Wang, C.; George, L.; Wuhner, R. Thermal and Pyrolysis Kinetics Analysis of Glass Wool and XPS Insulation Materials Used in High-Rise Buildings. *Fire* **2023**, *6*, 231. [[CrossRef](#)]
22. Zhang, D.; Xie, L.; Li, B. Effects of Nano-Nickel Oxide on Thermokinetics, Thermal Safety, and Gas-Generating Characteristics of 5-Aminotetrazole Thermal Degradation. *Fire* **2023**, *6*, 172. [[CrossRef](#)]
23. Yan, H.; Zhu, G.; Zhao, Y. Study on Pyrolysis Characteristics of Chinese Fir under Different Natural Aging Times. *Fire* **2022**, *5*, 161. [[CrossRef](#)]
24. Blaine, R.L.; Kissinger, H.E. Homer Kissinger and the Kissinger equation. *Thermochim. Acta* **2012**, *540*, 1–6. [[CrossRef](#)]
25. Boswell, P. On the calculation of activation energies using a modified Kissinger method. *J. Therm. Anal. Calorim.* **1980**, *18*, 353–358. [[CrossRef](#)]
26. Tian, B.; Qiao, Y.; Tian, Y.; Liu, Q. Investigation on the effect of particle size and heating rate on pyrolysis characteristics of a bituminous coal by TG–FTIR. *J. Anal. Appl. Pyrolysis* **2016**, *121*, 376–386. [[CrossRef](#)]
27. Jia, C.; Chen, J.; Liang, J.; Song, S.; Liu, K.; Jiang, A.; Wang, Q. Pyrolysis characteristics and kinetic analysis of rice husk. *J. Therm. Anal. Calorim.* **2020**, *139*, 577–587. [[CrossRef](#)]
28. Chen, J.; Fan, X.; Jiang, B.; Mu, L.; Yao, P.; Yin, H.; Song, X. Pyrolysis of oil-plant wastes in a TGA and a fixed-bed reactor: Thermochemical behaviors, kinetics, and products characterization. *Bioresour. Technol.* **2015**, *192*, 592–602. [[CrossRef](#)]
29. Dhyani, V.; Kumar, J.; Bhaskar, T. Thermal decomposition kinetics of sorghum straw via thermogravimetric analysis. *Bioresour. Technol.* **2017**, *245*, 1122–1129. [[CrossRef](#)]
30. Menzinger, M.; Wolfgang, R. The meaning and use of the Arrhenius activation energy. *Angew. Chem. Int. Ed. Engl.* **1969**, *8*, 438–444. [[CrossRef](#)]
31. Alarie, Y. Toxicity of fire smoke. *Crit. Rev. Toxicol.* **2002**, *32*, 259–289. [[CrossRef](#)] [[PubMed](#)]
32. Moriana, R.; Zhang, Y.; Mischnick, P.; Li, J.; Ek, M. Thermal degradation behavior and kinetic analysis of spruce glucomannan and its methylated derivatives. *Carbohydr. Polym.* **2014**, *106*, 60–70. [[CrossRef](#)]

Disclaimer/Publisher’s Note: The statements, opinions and data contained in all publications are solely those of the individual author(s) and contributor(s) and not of MDPI and/or the editor(s). MDPI and/or the editor(s) disclaim responsibility for any injury to people or property resulting from any ideas, methods, instructions or products referred to in the content.